Progress In Electromagnetics Research C, Vol. 28, 239–255, 2012

SYNTHESIS, DESIGN AND IMPLEMENTATION OF ULTRA-WIDEBAND IMPULSE RADIO ACTIVE MMIC MATCHED FILTERS

J. Xia*, C. L. Law, and Y. Zhou

Positioning and Wireless Technology Center, Nanyang Technological University, Research Techno Plaza, 50 Nanyang Drive, 4th Storey Border X Block, Singapore 639815, Singapore

Abstract—In this paper, we present a comprehensive framework from synthesis to implementation of active matched filters for UWB Impulse Radio. The method delays and sums UWB pulses coherently to strengthen the signal over white Gaussian noise. Theoretical analysis shows that the signal peak is maximized against noise, and an arbitrary transfer function could be realized by adjusting filter parameters. To verify the concept, a four-stage matched filter operating in 3–5 GHz with 360 degrees phase delay is demonstrated first. It is implemented in a commercial 2-μm GaAs HBT process and achieves a power gain of 13.8 dB with a 10 dB bandwidth of 1.3 GHz. Based on a similar architecture, another design is presented but with only half of the delay. It has a power gain of 15.9 dB and a 10 dB bandwidth of 2.3 GHz. An advantage of the proposed method is a precise control of the impulse response that can be matched to either symmetrical or asymmetrical UWB pulses by taking a time domain design approach.

1. INTRODUCTION

One of ultra-wideband impulse radio's (UWB-IR) most attractive and promising applications is real time location system (RTLS). With a bandwidth of several gigahertz and a data rate usually below a Megahertz, it offers the highest temporal resolution at possibly the lowest center frequency and power consumption. New exciting applications, such as asset management, industrial process control, supply chain management, security and personnel monitoring, could

Received 1 October 2011, Accepted 3 November 2011, Scheduled 13 April 2012

* Corresponding author: Jingjing Xia (xiaj0003@e.ntu.edu.sg).

be achieved with better accuracy and, most importantly, in real time. Several commercial systems are available in the market [1–4] and research activities in this area are summarized in [5].

To co-exist with other narrowband technology, UWB signals are pseudo-randomly modulated and appear to be noise-like with a spectral density no greater than 50 nanoWatts/MHz. It is well known that a matched filter is the optimum estimator for time-of-arrival (TOA) in additive white Gaussian noise (AWGN) channel, in that it maximizes the output SNR and hence improves the ranging and positioning accuracy [6]. To improve the SNR of a UWB receiver, a matched filter could be used.

Despite the fact that many papers implemented matched filter in algorithm [6–9], reports of analog UWB matched filter are very limited. A few exceptions include: surface acoustic wave filter is used as an UWB matched filter in [10]. Reflection-mode transmission line can realize matched filtering as well [11]. In [12], a Chebyshev filter with its transfer function similar to the input spectrum is used. A tapped Microstrip delay line matched filter with Wilkinson power combiner is reported in [13]. In this study, synthesis of UWB active matched filter based on tapped delay line structure is proposed. This paper expands on some preliminary results presented in [14], with theory, synthesis method, design procedures, and analysis introduced in detail. To the author's best knowledge, this is the first paper in UWB-IR active matched filter with comprehensive descriptions.

2. PRINCIPLES OF OPERATION

2.1. Matched Filter in UWB-IR Pulses Detection

UWB waveform $s_i(t)$ is received and corrupted by a white noise $n_i(t)$, as in Figure 1. In a precision UWB localization system, one wishes to determine the presence of such pulses at certain time $t = t_1$ when the amplitude is getting considerably greater. The accuracy in estimating t_1 determines the overall positioning accuracy.

To maximize the signal while suppressing the noise as much as possible, one first thought is to have a rectangular shape bandpass filter (BPF), with maximal transmission in the passband and minimal transmission in the stopband. Whether feasible or not to realize such a filter, one question pertaining to the design of such a filter is the choice of the bandwidth (B_F). UWB-IR signal usually has a non-flat spectrum with a bandwidth in gigahertz range. It will be shown that, in case of a BPF, there indeed exists an optimal B_F that maximizes the signal to noise ratio (SNR).

Unlike a bandpass filter that has a rectangular shape response, a matched filter has a transfer function that is the complex conjugate of the spectrum of the input signal, or $H(f) = S^*(f)$. Such a response could maximize the transmission at frequencies where the signal is large compared to the noise, and minimize the transmission when the signal is small compared to noise. Therefore it strengthens the signal against white noise and is often regarded as the optimal filter to maximize the SNR.

To quantitatively understand why a matched filter is *the optimal* filter in maximizing SNR when compared with a bandpass filters, calculations were done in MATLAB to evaluate its signal and noise performance. One should note that the input UWB waveform is taken from our previous work [15].

As a linear filter, output from a matched filter in Figure 1 can be decomposed into output signal $s_o(t)$, due to input signal $s_i(t)$ only, and output noise $n_o(t)$, due to input noise $n_i(t)$ only. For the signal $s_i(t)$, the output is

$$s_o(t) = \int_0^t s_i(\tau)h(t-\tau)d\tau \tag{1}$$

Similarly for the input noise $n_i(t)$, the output is

$$n_o(t) = \int_0^t n_i(\tau)h(t-\tau)d\tau \tag{2}$$

For simplicity, we assume a perfect synchronization and sample at $t = t_1$. A UWB matched filter intends to maximize the magnitude of detected pulses at $t = t_1$ against the noise at that instant. The output

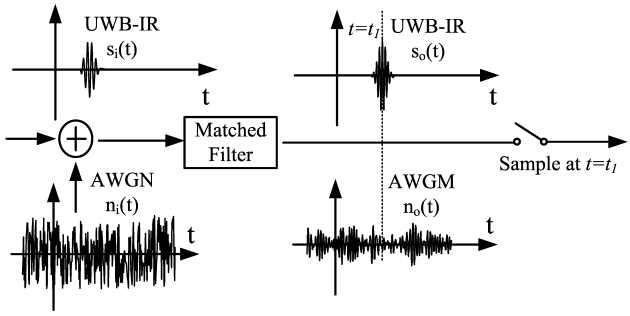

Figure 1. Scenario pertaining to the maximization of signal-to-noise ratio.

signal-to-noise ratio is defined accordingly as

$$SNR_o = \left(\frac{s_o(t = t_1)}{rms(n_o(t = t_1))} \right)^2 \tag{3}$$

To provide a benchmark, three types of classic analogue bandpass filters (BPFs), Butterworth, Chebyshev and elliptical, are synthesized with transfer functions expressed in poles and zeros, or

$$H_{BPF}(f) = \prod_1^N (jf - z_i) \; / \; \prod_1^N (jf - p_i) \tag{4}$$

A bandwidth (B_F) of 2 GHz at the center frequency 4 GHz is chosen for the BPFs, which corresponds to the 10 dB bandwidth of our UWB waveform. Figure 2 compares transfer functions of the matched filter with the BPFs. It is obvious a matched filter has the distinct feature of resembling the input signal spectrum while BPFs try to achieve a brick wall-like passband.

With (1)–(4), the output SNR of the matched filter are normalized and compared with BPFs in Figure 3. The result indicates that SNR_o of a matched filter could outperform the BPFs by as much as 1.6 dB

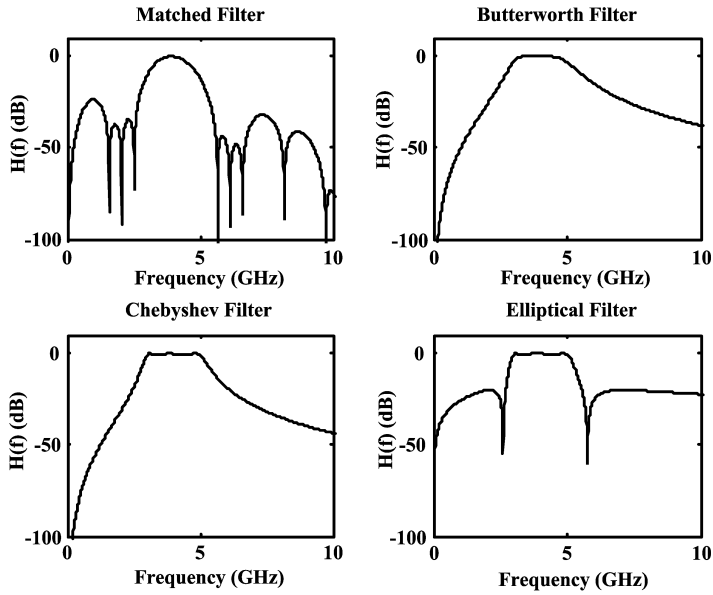

Figure 2. Comparison of transfer functions between a matched filter and "brick wall-like" bandpass filters.

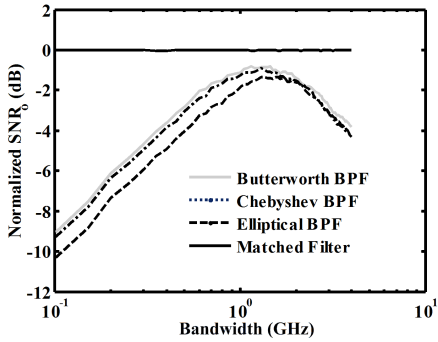

Figure 3. SNR comparison between a matched filter and ideal bandpass filters with different bandwidth.

at 2 GHz. Butterworth filter, with a slower roll-off, has surprisingly achieved a better SNR than Chebyshev or elliptical filters. If B_F is reduced to 1.3 GHz which is the optimal in SNR but with slight signal distortion, a matched filter is still better off than the BPFs.

Compared with BPFs with any B_F, matched filter indicates a better SNR_o. Therefore it can be concluded that a matched filter is the optimal filter in maximizing SNR in UWB pulses detections. The advantages of a matched filter also include: 1. in case of in-band narrow band interference, a matched filter is still able to improve its signal-to-interference ratio while other methods are incapable of; 2. in case of an asymmetrical UWB pulse shape in the time domain, its matched filter can be easily synthesized in the time domain while frequency domain synthesis are more difficult.

2.2. Synthesis of Arbitrary UWB-IR Matched Filter

Synthesis of a matched filter was discussed in the classic work by Turin using tapped delay line structures [16]. The block diagram is shown in Figure 4. The response of such a filter depends on the choice of three parameters, which are delay D_1, filter coefficient a_k, and band limiting filter $F(j\omega)$. Its transfer function is given by

$$H(j\omega) = F(j\omega) \sum_{k=0}^{N-1} a_k \exp(-jk\omega D_1) \tag{5}$$

By adjusting the delay D_1, we are able to arrange the signals to be added up in phase. In the meanwhile, the white Gaussian noise at the input is added up non-coherently. In the ideal case where a noise-free N-tap matched filter is assumed, the signal increases $\sqrt{N}$ times

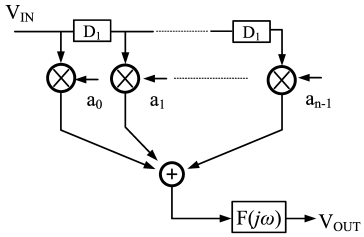

Figure 4. Block diagram to synthesize arbitrary UWB matched filter.

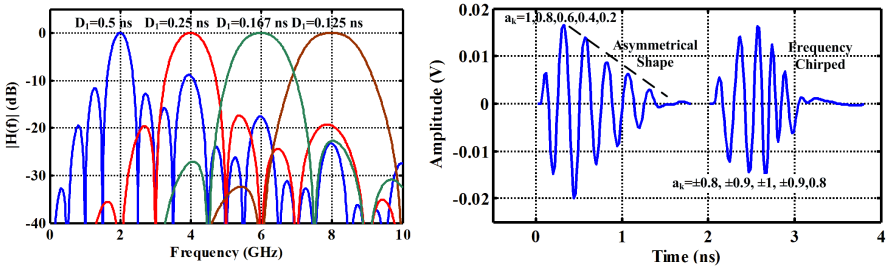

(a) (b)

Figure 5. (a) Synthesized transfer functions at different frequency and (b) Synthesized impulse response for special UWB waveforms.

faster than the root-mean-squared (*rms*) of the noise. By adjusting the number of stages N and filter coefficients a_k, filter bandwidth and out of band shape can be changed. One should note there is also a transmission peak for every 2π off the center frequency. Therefore a simple low-order band-pass filter could be used for $F(j\omega)$ to reject harmonics. In Figure 5(a), matched filters at different centre frequency are plotted using this method.

Non-uniform waveforms, such asymmetrical envelop or frequency chirped pulses are not rare in a UWB-IR system. In Figure 5(b), impulse responses for such pulses are synthesized and plotted. In the following sections, UWB matched filters will be presented using the proposed method.

3. FOUR STAGES MATCHED FILTER

3.1. Circuit Design and Analysis

A straightforward way to synthesize a match filter is to let D_1 equal to 360 degrees at the center frequency, a_k with the same sign and value

and $F(j\omega)$ be bandpass. A circuit to realize the proposed diagram is shown in Figure 6. It consists of two parts: input stage and gain stage. The input section is a combination of artificial line and transmission line. Constant-k sections (L_B, C_B) absorb the intrinsic base-emitter capacitance (C_{be}) and forms an artificial transmission line. An off-chip delay line is inserted between the constant-k sections for the delay.

It is our interest here to find the voltage and its phase at each stage where it is tapped, or V_k ($k = 1$ to 4) in Figure 6. A single section of a simplified small signal model is shown in Figure 7, where R_{be} is the total base resistance. A reasonable assumption we made is the reflection can be neglected if the characteristic impedance of artificial transmission line (Z_k) and transmission line (Z_0) is matched and terminated by R_B, or

$$Z_k = \sqrt{\frac{L_B}{C_B // C_{be}}} = Z_0 = R_B \tag{6}$$

It gives a good estimation below the cut-off frequency and better accuracy can be achieved later on through the simulator.

At the k-th stage, V_k is related to the input voltage V_{in} through the propagation constant γ_k, or

$$V_k = V_{in} \exp(-j\gamma_k) \tag{7}$$

where $\gamma_k = (2k-1)/2\gamma_1 + (k-1)\gamma_2$, γ_1 and γ_2 are the propagation constant of the constant-k section and transmission line respectively.

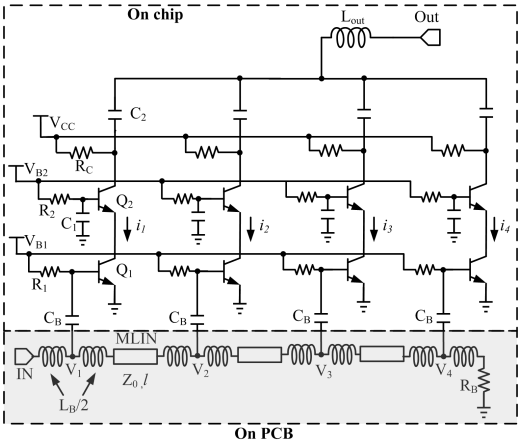

Figure 6. Schematic of the four stages matched filter.

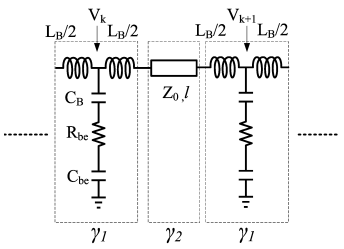

Figure 7. Equivalent small signal model of the base line.

For γ_1,

$$\gamma_1 = \alpha_1 + j\beta_1 \tag{8}$$

where α_1, with a real part in the equation, contributes to the attenuation and β_1, being the imaginary part, is the phase delay. With image impedance method, β_1 and α_1 can be expressed as

$$\beta_1 \approx 2\sin^{-1}(\omega/\omega_c) \tag{9}$$

$$\alpha_1 = \frac{(\omega_c/\omega_b)X^2}{\sqrt{1-[1-(\omega_c/\omega_b)^2]X^2}} \tag{10}$$

where $\omega_c = 2/\sqrt{L_B C}$, $\omega_b = 1/R_{be}C$, $X = \omega/w_c$ and $C = C_B//C_{be}$.

Similarly for the transmission line, its propagation constant is given by

$$\gamma_2 = \alpha_2 + j\beta_2 \tag{11}$$

$$\beta_2 = \omega l\sqrt{\varepsilon_{eff}}/c \tag{12}$$

Since α_2 is a parameter highly dependent on the substrate and its contribution is less significant than α_1, it is neglected in the analysis.

With (9) and (12), to have a phase delay of 360 degrees at the center frequency between two consecutive stages, we need

$$\angle(\gamma_{i+1} - \gamma_i) = 2\sin^{-1}(\omega/\omega_c) + \omega l\sqrt{\varepsilon_{eff}}/c = 2\pi \tag{13}$$

There are only two unknown variables in (13), which are the cut-off frequency ω_c and delay line length l. The cut-off frequency should be relatively far from the operation frequency (3–5 GHz) and an initial value is assumed (15 GHz). Based on this, L_B, C_B and l could be found accordingly.

There are two purposes in the gain stage: firstly, the gain stage sets the filter coefficient at each tap and compensates for the losses due to the input stage; secondly, the gain stage converts the voltages tapped into currents and combines them at the output. In this design, cascoded HBT transistors (Q_1 and Q_2) are used as the gain stage. With equal filter coefficients, gm is increased in the latter stages to compensate losses from previous stages. By combining all currents from gain stages, the output voltage is given by

$$\begin{aligned} V_{out} &= \sum_{k=0}^{3} i_k \frac{R_c R_{out}}{R_c + R_{out} + 1/sC_2 + sL_{out}} \\ &= v_{in} T \sum_{k=0}^{3} gm_k \exp\left[-\frac{2k+1}{k}(\alpha_1 + j\beta_1)\right] \exp(-jk\beta_2) \end{aligned} \tag{14}$$

where

$$T = \frac{C_B}{C_B + C_{be} + s^2 R_{be}} \frac{R_c R_{out}}{R_c + R_{out} + 1/sC_2 + sL_{out}} \tag{15}$$

C_{be}, R_{be} and gm in the equation is extracted from the vendor's VBIC large signal model. The analysis will be verified with simulation and measurement in the following text.

3.2. Co-simulation of Delay Line and Circuits

The delay line is implemented as stripline on a multi-layer PCB board. Its layout and layer stackup is shown in Figure 8. The delaylines are highlighted in blue with a length of 33 mm each. The complexity in the chip-PCB interface leads to some design difficulties including: 1. Parasitic coupling and inductance from PCB traces; 2. Accurate prediction of bonding wire inductance. EM and circuit co-simulation is used to take these into considerations [17].

The simulated return loss (S_{11}) of Figure 6 is plotted in Figure 9 with bonding wire length varied from 0.5 mm to 1.5 mm. The figure shows a bonding wire of 0.75 mm gives the best overall impedance matching. The reflection is significant when the wire is below 0.5 mm or above 1 mm.

To assess the loss when the delay line is loaded by the HBTs, insertion loss between input and base terminating resistor (R_B) is simulated and plotted in Figure 10. The minimal insertion loss is 2 dB at 4 GHz with a bonding wire of 0.75 mm. The loss reduces to 0.8 dB without the HBT, which verifies that constant-k section dominates the loss over the transmission lines.

To better understand the principles of the proposed matched filter, simulated output current $i_1 - i_4$ (Figure 6) are plotted in Figure 11. Current from each stage is delayed by 360° to be coherent while noise is random and non-coherent. Once combined, the signal is amplified more than the noise.

An analog matched filter should have a transfer function similar to the input waveform spectrum and a noise figure of a LNA. One of the major noise contributors is the base line terminating resistor R_B. A larger R_B (> 50 Ohm) reduces the overall noise, but at the

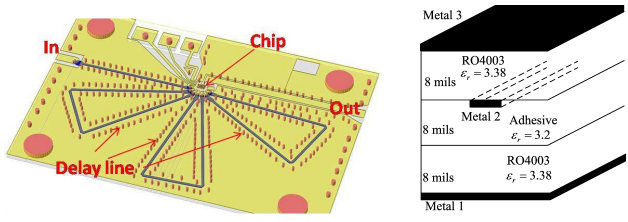

Figure 8. Delay line layout in Stripline and layer stackup.

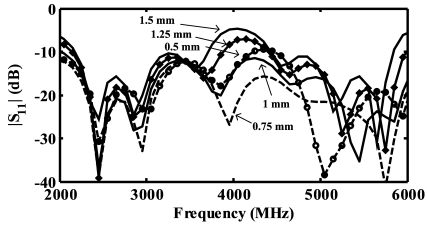

Figure 9. Full-wave EM simulation of the return loss $|S_{11}|$ with different bonding wire length.

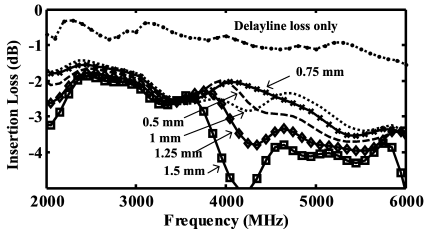

Figure 10. Simulated insertion loss of the delay line with different bonding wire length.

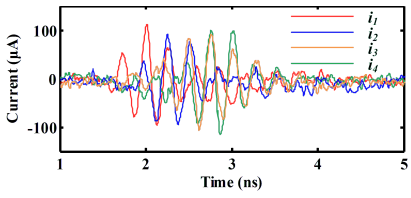

Figure 11. Simulated transient current at each tap for the four stages matched filter.

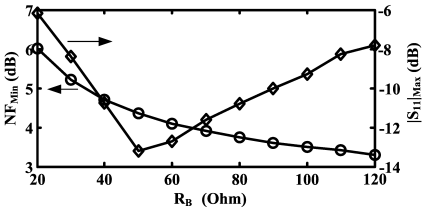

Figure 12. Simulated noise figure and S_{11} at different R_B.

expense of impedance mismatch. The trade-off between noise figure and S_{11} between 3–5 GHz as a function of R_B is plotted in Figure 12. The figure indicates that increasing R_B to 100 Ohm reduces the noise figure to 3.6 dB with an acceptable S_{11}.

3.3. Measurement

Figure 13 shows the microphotograph of the designed chip with an area of 1 mm×1 mm. The chip is fabricated in a commercial 2-μm GaAs HBT process with a cut-off frequency f_T of 33 GHz. The chip is wire bonded to the PCB and measured using SMA connectors.

It is biased from 3.3 V supply and consumes 12.1 mA current. The S-Parameters are measured using an Agilent N5244A PNA and plotted in Figures 14 and 15. The measured power gain (S_{21}) matches well with EM simulation. It has a peak gain of 13.8 dB at 4 GHz. The gain rolls off as frequency increases or decreases from the center frequency, and transmission zeros occurs every 1 GHz. The calculated gain using (14) is plotted in the same figure. Good agreement is achieved between

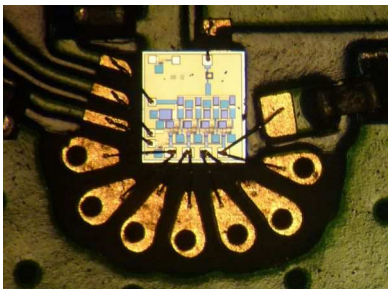

Figure 13. Microphotograph of the fabricated chip wire bonded to PCB. The chip size is 1 mm × 1 mm.

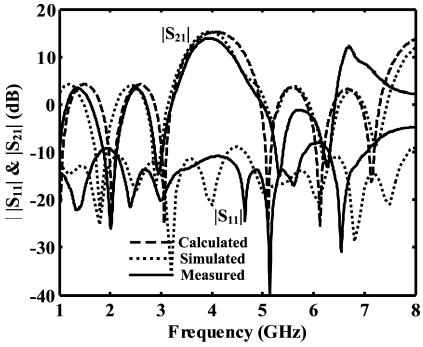

Figure 14. Measured (solid line) and simulated (dotted line) $|S_{11}|$ and $|S_{21}|$ of the four stages matched filter. The calculated $|S_{21}|$ is also plotted in dashed line.

Table 1. Parameters for the calculation of gain.

$R_{be} = 12.5\,\text{Ohm}$	$C_{be} = 0.8\,\text{pF}$
$C_B = 0.7\,\text{pF}$	$L_B = 0.65\,\text{nH}$
$l = 38\,\text{mm}$	$R_c = 300\,\text{Ohm}$
$R_{out} = 50\,\text{Ohm}$	$C_2 = 2\,\text{pF}$
$L_{out} = 1\,\text{nH}$	$\varepsilon_{eff} = 3.38$
$gm_k = 0.1, 0.103, 0.105, 0.108$	

our theory, simulation and measurement. All the parameters used to calculate the gain is listed in Table 1. The measured input return loss (S_{11}) is better than −10.9 dB and output return loss (S_{22}) is better than −12.2 dB from 3–5 GHz. The reverse isolation (S_{12}) is smaller than −28 dB.

Noise figure (NF) is measured using a HP 8970B noise meter and plotted in Figure 16. It has a NF of 4.2 dB at the center frequency of 4 GHz, slightly higher than the simulated value of 3.7 dB. The NF increases when frequency is away from 4 GHz, due to a reduced gain. Linearity was evaluated using input 1-dB compression point ($\text{IP}_{1\,\text{dB}}$) instead of third-order intercept point (IIP3) as IR-UWB is occupying a single band instead of hopping between different channels. The measured input $\text{IP}_{1\,\text{dB}}$ is −3.1 dBm at 4 GHz.

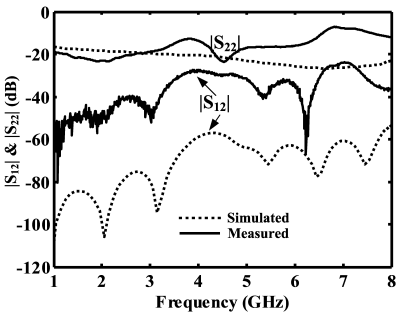

Figure 15. Measured (solid line) and simulated (dotted line) $|S_{12}|$ and $|S_{22}|$.

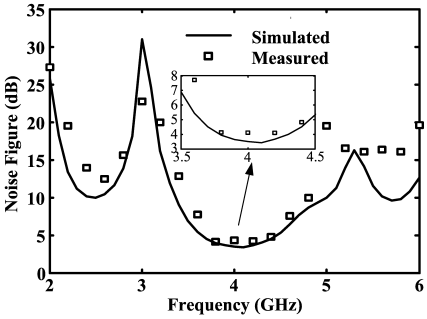

Figure 16. Measured (square dots) and simulated (solid line) noise figure.

4. FIVE STAGES MATCHED FILTER

4.1. Circuit Design, Analysis and Simulation

In the last section, one full cycle delay line at 4 GHz is used. The delay line introduces losses as well as noise, and its length should be minimized. Tapping an arbitrary delay, e.g., 45 degrees, could actually be compensated by the gain stages (with 315 degrees phase shift in this case) and still maintain the coherency. Since a transistor can be either inverting or non-inverting, a delay of 180 degrees is used between input stage and the remaining 180 degrees will be from the gain stage. Other filter parameters remain similar to the previous design.

Circuit implementation of the desired function is shown in Figure 17. Differences from the previous design include: 1. Delay line length l is reduced by half; 2. inverting and non-inverting amplifiers are alternating. Transistors (Q_1 and Q_2) are cascoded to form the inverting amplifier with a transconductance $gm^- \approx -gm_{Q1}$. Two current-reuse common emitter stages (Q_3 and Q_4) are cascaded to achieve a positive amplification. Capacitor C_3 provides the AC ground to the emitter of Q_4 and R_5 provides the DC path. Its transconductance is given by

$$gm^+ = \frac{i}{V_{b3}} = \frac{gm_{Q3}gm_{Q4}R_C C_2}{C_2 + C_{be4} + j\omega C_2 C_{b4}(R_5 + R_{be4})} \tag{16}$$

Equations (6)–(13) from the previous section could be reused to calculate the gain. By combining all currents from the gain stages, the voltage gain is given by

$$A_v = T\sum_{k=0}^{4} gm_k \exp\left[-\frac{2k+1}{k}(\alpha_1 + j\beta_1)\right]\exp(-jk\beta_2) \tag{17}$$

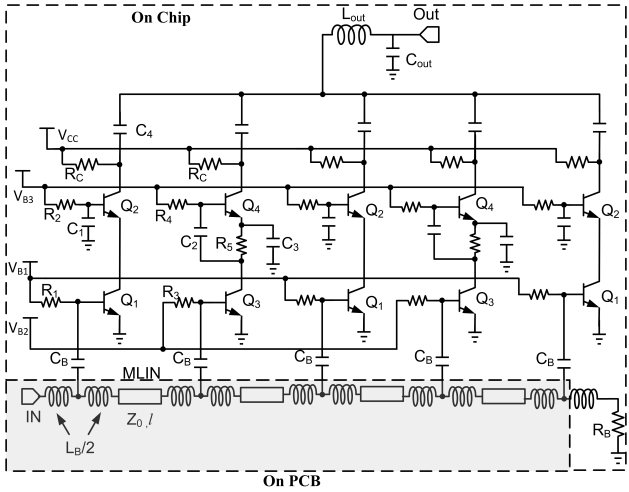

Figure 17. Schematic of the five stages matched filter.

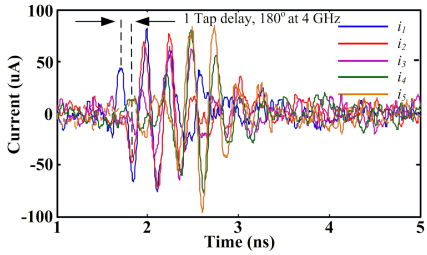

Figure 18. Simulated transient current at each tap for the five stages matched filter.

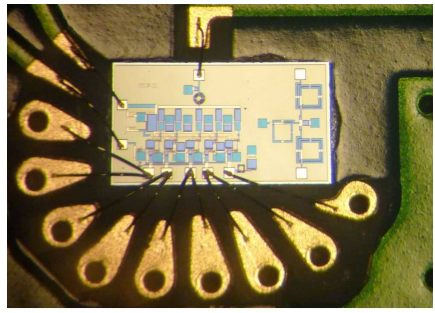

Figure 19. Microphotograph of the fabricated chip wire bonded to PCB.

where

$$T \approx \frac{C_B}{C_B + C_{be} + s^2 R_{be}} \frac{R_c R_{out}}{R_c + R_{out} + 1/sC_4 + sL_{out}} \tag{18}$$

The analysis will be verified with simulation and measurement in the following text. EM and circuit co-simulation is similar to the last section and will not be discussed here.

Output currents $i_1 - i_5$ (Figure 17) are simulated and plotted in Figure 18. Current from each stage is delayed by 180° and flipped to be coherent. This is distinct from the last section where each tap is

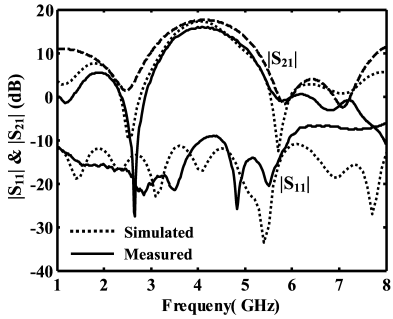

Figure 20. Measured (solid line) and simulated (dotted line) $|S_{11}|$ and $|S_{21}|$ of the five stages matched filter. The calculated $|S_{21}|$ is also plotted in dashed line.

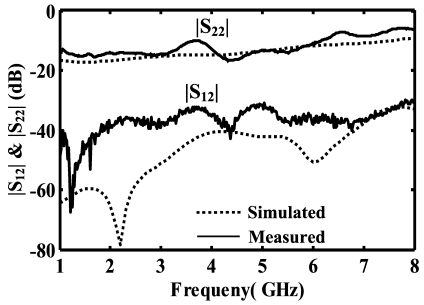

Figure 21. Measured (solid line) and simulated (dotted line) $|S_{12}|$ and $|S_{22}|$ of the five stages matched filter.

separated by a full cycle. It is important to equalize the magnitude of currents at each tap. The gain of a cascaded stage is normally much higher than a cascoded stage. To let $gm^- = gm^+$, (16) can be simplified to $gm^+ \approx gm_{Q3}gm_{Q4}R_C$ for a first order analysis. Reducing the tansconductance of Q_3 and Q_4 by lowering the bias current could equalize the tap gain. However the base resistance and loss will increase accordingly. In the final design, the non-inverting stage is biased at half the current of the inverting stage and R in (16) is adjusted accordingly for equal tap gain.

4.2. Measurement and Discussion

Figure 19 shows the microphotograph of the designed chip wire bonded to a PCB. The chip size is 1 mm × 2 mm and is biased from a 3.3 V supply at 15.3 mA current.

The measured S-Parameters are plotted in Figures 20 and 21. The measured S_{21} agrees well with simulation and has a peak gain of 15.9 dB at 4 GHz. Compared with the four stages matched filter, its transfer function has transmission zeros which are separated further with a wider bandwidth. The calculated transfer function in (17) showed good agreement in Figure 20 as well. Values of all the parameters used in the calculation are listed in Table 2. The measured input return loss (S_{11}) is better than −9 dB and output return loss (S_{22}) is better than −11.4 dB from 3–5 GHz. The reverse isolation (S_{12}) is smaller than −31.5 dB.

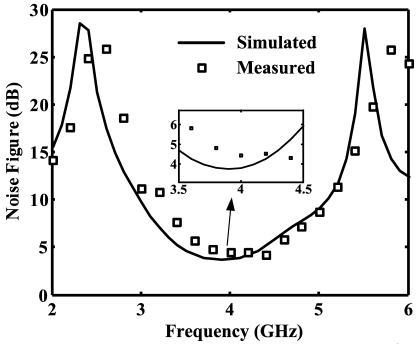

Figure 22. Measured (square dots) and simulated (solid line) noise figure of the five stages matched filter.

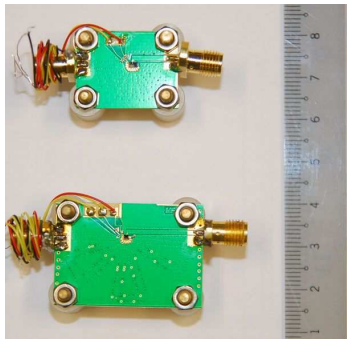

Figure 23. PCB test board for both designs.

Table 2. Parameters for the calculation of gain.

$R_{be1} = 12.5\,\text{Ohm}$	$C_{be1} = 0.8\,\text{pF}$	$C_B = 0.7\,\text{pF}$
$R_{be3} = R_{be4} = 15.3\,\text{Ohm}$	$C_{be3} = C_{be4} = 0.95\,\text{pF}$	$L_B = 0.7\,\text{nH}$
$l = 18\,\text{mm}$	$R_c = 300\,\text{Ohm}$	$C_4 = 2\,\text{pF}$
$R_{out} = 50\,\text{Ohm}$	$L_{out} = 1\,\text{nH}$	$\varepsilon_{eff} = 3.38$
$gm_0 = -0.1$, $gm_2 = -0.105$, $gm_4 = -0.11$		$gm_{Q3} = gm_{Q4} = 0.055$

The noise figure is measured using a HP 8970B noise meter and plotted in Figure 22. It has a noise figure of 4.5 dB at the centre frequency of 4 GHz. Comparing with the previous section, the noise figure is slightly higher since five stages are used. The measured input 1-dB compression point ($\text{IP}_{1\,\text{dB}}$) is -15 dBm. The $\text{IP}_{1\,\text{dB}}$ is lower than the previous design, due to a lower bias current in the non-inverting stages.

A photograph of both designs with test boards is shown in Figure 23. Since the delay line is reduced by half, the five stages matched filter takes only 40% of the overall size as compared with the four stages design.

5. CONCLUSION

A novel matched filter synthesis suitable for UWB-IR has been introduced in this paper. It is based on a tapped delay line structure, which delays and sums UWB-IR pulses coherently to achieve a

positive gain over the white noise. Two different matched filters are implemented in a low cost 2-μm GaAs HBT process and our concept is verified through experiment. It is worth mentioning that this tapped delay line structure is used in our previous work to generate the UWB signals as well [16, 18]. Similarity between the input signal and the matched filter could be maximized using this approach.

REFERENCES

1. Ubisense Real-time Location Systems (RTLS), Ubisense, Cambridge, U.K. [Online]. Available: http://www.ubisense.net/en/rtls-solutions.
2. Time Domain's Ultra Wideband (UWB) Definition and Advantages, Time Domain Corp., Huntsville, AL, [Online]. Available: http://www.timedomain.com.
3. Dart UWB Hub & Sensors, Zebra Technologies [Online]. Available: http://www.zebra.com.
4. DecaWave ScenSor Product Brief, Decawave, Dublin, Ireland, [Online]. Available: http://www.decawave.com/downloads1.html.
5. Kuhn, M. J., M. R. Mahfouz, C. Zhang, B. C. Merkl, and A. E. Fathy, "A system-level simulation framework for UWB localization," *IEEE Trans. Microw. Theory Tech.*, Vol. 58, No. 12, 3527–3537, Dec. 2010.
6. Dardari, D., A. Conti, U. Ferner, A. Giorgetti, and M. Z. Win, "Ranging with ultrawide bandwidth signals in multipath environments," *Proc. IEEE*, Vol. 97, No. 2, 404–426, Feb. 2009.
7. Low, Z. N., J. H. Cheong, C. L. Law, W. T. Ng, and Y. J. Lee, "Pulse detection algorithm for line-of-sight (LOS) UWB ranging applications," *IEEE Antennas Wireless Propag. Lett.*, Vol. 4, 63–67, Jun. 2005.
8. Redfield, R., S. Ye, and H. Liu, "High-precision indoor UWB localization: Technical challenges and method," *Proc. IEEE Int. Conf. Ultra-wideband*, 1–4, Sep. 2010.
9. Yen, N. Y. and S. L. Su, "Robust matched-filter acquisition for direct-sequence ultrawideband systems," *IEEE Trans. Veh. Technol.*, Vol. 58, No. 8, 4419–4425, Aug. 2009.
10. Brocato, R., E. Heller, J. Wendt, J. Blaich, G. Wouters, E. Gurule, G. Omdahl, and D. Palmer, "UWB communication using SAW correlators," *Proc. IEEE Radio and Wireless Symp.*, 267–270, Sep. 2004.

11. Arnedo, I., I. Arregui, M. Chudzik, A. Lujambio, M. A. G. Laso, T. Lopetegi, J. D. Schwartz, J. Azana, D. V. Plant, and IEEE, "Arbitrary UWB pulse generation and optimum matched-filter reception," *Proc. IEEE Int. Conf. Ultra-wideband*, 43–48, New York, Sep. 2009.
12. Kawano, Y., Y. Nakasha, K. Yokoo, S. Masuda, T. Takahashi, T. Hirose, Y. Oishi, and K. Hamaguchi, "RF chipset for impulse UWB radar using 0.13-μm InP-HEMT technology," *IEEE Trans. Microw. Theory Tech.*, Vol. 54, No. 12, 4489–4497, Dec. 2006.
13. Xia, J., C. L. Law, and J. Jiang, "A novel 3–5 GHz active matched filter for impulse radio ultra-wideband," *IEEE Microw. Wireless Compon. Lett.*, Vol. 19, No. 7, 458–460, Jul. 2009.
14. Xia, J., C. L. Law, and Y. Zhou, "Synthesis and design of novel active MMIC matched filters for ultrawideband impulse radio," *IEEE MTT-S Int. Microw. Symp. Dig.*, Baltimore, MD, Jun. 2011.
15. Xia, J., C. L. Law, Y. Zhou, and K. S. Koh, "3-5 GHz UWB impulse radio transmitter and receiver MMIC optimized for long range precision wireless sensor networks," *IEEE Trans. Microw. Theory Tech.*, Vol. 58, No. 12, 4040–4051, Dec. 2010.
16. Turin, G., "An introduction to matched filters," *IRE Trans. Inf. Theory*, Vol. 6, No. 3, 311–329, Mar. 1960.
17. AWR AXIEM Extract Flow White Paper, AWR Corp, [Online]. Available: http://web.awrcorp.com.
18. Fang, C., C. L. Law, J. C. M. Hwang, and J. Xia, "Design and analysis of high-voltage high-efficiency ultra-wideband pulse synthesizer," *Progress In Electromagnetics Research C*, Vol. 20, 187–201, 2011.